Sulfur K-edge micro- and full-field XANES identify marker for preparation method of ultramarine pigment from lapis lazuli in historical paints

Alessa A. Gambardella, Marine Cotte, Wout de Nolf, Kokkie Schnetz, Rob Erdmann, Roel van Elsas, Victor Gonzalez, Arie Wallert, Piet D. Iedema, Myriam Eveno, et al.

CHEMISTRY

Sulfur K-edge micro- and full-field XANES identify marker for preparation method of ultramarine pigment from lapis lazuli in historical paints

Alessa A. Gambardella[1]*, Marine Cotte[2,3†], Wout de Nolf[2†], Kokkie Schnetz[4], Rob Erdmann[1,5], Roel van Elsas[6], Victor Gonzalez[1], Arie Wallert[1], Piet D. Iedema[4], Myriam Eveno[7,8], Katrien Keune[1,4]

Ultramarine blue pigment, one of the most valued natural artist's pigments, historically was prepared from lapis lazuli rock following various treatments; however, little is understood about why or how to distinguish such a posteriori on paintings. X-ray absorption near-edge structure spectroscopy at the sulfur K-edge in microbeam and full-field modes (analyzed with nonnegative matrix factorization) is used to monitor the changes in the sulfur species within lazurite following one such historically relevant treatment: heating of lapis lazuli before extracting lazurite. Sulfur signatures in lazurite show dependence on the heat treatment of lapis lazuli from which it is derived. Peaks attributed to contributions from the trisulfur radical—responsible for the blue color of lazurite—increase in relative intensity with heat treatment paralleled by an intensified blue hue. Matching spectra were identified on lazurite particles from five historical paint samples, providing a marker for artists' pigments that had been extracted from heat-treated lapis lazuli.

INTRODUCTION

Ultramarine blue is a pigment composed of the blue mineral lazurite, the most prominent component of the semi-precious stone lapis lazuli. Historically, the most commonly documented source of lapis lazuli is modern-day Afghanistan, particularly the Sar-e-Sang deposit within the Badakhshan region (*1*–*4*); recently, other sources have been considered as well (*3*, *5*). Highly valued for its vibrant color, ultramarine has been used in artworks for centuries, and it was eventually produced synthetically for the first time in the early 19th century (*1*, *2*, *6*).

Lazurite, typically approximated as $(NaCa)_8[Al_6Si_6O_{24}](SO_4,S,Cl)_2$ (*1*, *7*), has an aluminosilicate cage structure known as a beta (β) cage, within which the cations and anions are found (*8*). As a member of the sodalite group of minerals, lazurite shares strong similarities to sodalite ($Na_8[Al_6Si_6O_{24}](Cl_2)$), nosean ($Na_8[Al_6Si_6O_{24}](SO_4)\cdot H_2O$), and haüyne ($(Na,Ca)_{4-8}[Al_6Si_6O_{24}](SO_4,S,Cl)_{1-2}$) (*7*), with lazurite often considered as a sulfide-rich form of the last (*3*). The color of lazurite has been attributed, in particular, to the sulfur radical species trapped within the cage where di-, tri-, and tetrasulfur radicals are proposed to contribute to yellow, blue, and red hues, respectively; the presence of the lattermost radical is still debated (*9*–*21*).

Before the availability of the synthetic form, lazurite was extracted from lapis lazuli as early as the 13th century, a process motivated by a desire for the deepest blue hue (*22*–*24*). Recipes called for intricate extraction methods to isolate lazurite from accessory minerals of lapis lazuli, such as pyrite (FeS_2), calcite ($CaCO_3$), diopside ($MgCaSi_2O_6$), or wollastonite ($CaSiO_3$) (*1*, *6*). These typically involved kneading ground lapis lazuli rock within a "dough" known as "pastello," often comprising resins, beeswax, and oil (*22*, *25*–*28*). This traditional pastello extraction is described in detail in Cennino Cennini's Il Libro dell'Arte (*23*) and has been the subject of recent studies with the aim to better understand its selection for lazurite (*22*, *29*).

Through historical documents, it is further clear that artists were known to obtain or prepare their pigments in different ways (*22*, *25*–*28*). Specifically, some recipes instruct heating the lapis lazuli rock with fire or until "red hot" before grinding into a powder and extracting lazurite (*25*, *27*). There are also reports indicating the exposure of lapis lazuli to heat through mining practices known as "fire setting" dating as early as antiquity (*4*, *30*, *31*). Previous research on lazurite powder has demonstrated that various properties of lazurite change with heat (*32*–*36*), including the size of the β cage (*32*) as well as the sulfur speciation and correlating color (*33*–*35*), and that the extent of these changes is influenced by temperature, duration, and access to oxygen. To date, however, these properties, to our knowledge, have not yet been studied for lazurite pigment derived from heat-treated rock but rather only from heat-treated powders.

Motivated by previous reports, this study seeks to determine whether sulfur chemistry—as influenced by heat treatment—provides a unique marker for the historical treatment of lazurite, or ultramarine, used in paintings. Such a marker would contribute to technical art history, aiding our understanding of the use of the most highly valued pigment throughout history. Furthermore, ultramarine-based paints (e.g., mixed with a drying oil) are known to show "ultramarine disease," a degradation phenomenon that markedly changes the aesthetic and integrity of the artwork, showing apparent color changes at the surface (*1*, *25*). Degradation does not always occur. We suspect that these treatments affect the susceptibility of ultramarine-based paints to degradation; therefore, finding a marker for pigment

[1]Rijksmuseum, Conservation and Science, Hobbemastraat 22, 1071 ZC, Amsterdam, Netherlands. [2]European Synchrotron Radiation Facility (ESRF), 71 Avenue des Martyrs, 38000 Grenoble, France. [3]Sorbonne Université, CNRS, Laboratoire d'Archeologie Moléculaire et Structurale, LAMS, 4 place Jussieu, 75005 Paris, France. [4]Van't Hoff Institute for Molecular Sciences, University of Amsterdam, Science Park 904, 1090 GD, Amsterdam, Netherlands. [5]Conservation and Restoration, University of Amsterdam, Johannes Vermeerplein 1, 1071 DV, Amsterdam, Netherlands. [6]Vrije Universiteit, De Boelelaan 1105, 1081 HV, Amsterdam, Netherlands. [7]Centre de Recherche et de Restauration de Musées de France (C2RMF), 14 Quai François Mitterrand, Palais du Louvre, 75001 Paris, France. [8]PSL Research University, Chimie ParisTech—CNRS, Institut de Recherche Chimie Paris, UMR8247, 75005 Paris, France.
*Corresponding author. Email: aagambardella@gmail.com
†These authors contributed equally to this work.

preparation is a first step toward determining a method to treat ultramarine disease.

Using x-ray absorption near-edge structure (XANES) spectroscopy at the sulfur K-edge, sulfur speciation is measurable and variation observable. Sensitive to the oxidation state and coordination chemistry of sulfur species (*37*, *38*), XANES provides specific information about sulfur species, complementary to other techniques commonly used on ultramarine such as Raman (*9*, *10*, *14*, *39*), Fourier transform infrared (*36*, *40*), and nuclear magnetic resonance spectroscopy (*11*, *13*). In addition to being sensitive to heat treatment—as demonstrated by Tauson *et al.* (*33*) and Fleet and Liu (*34*) on heated lazurite powder—sulfur speciation of ultramarine/lazurite as measured by XANES also depends on geographical provenance (*41*) and stage of extraction (*29*) for natural lazurite as well as conditions of synthesis for synthetic ultramarine (*7*, *34*, *42*).

Here, XANES via microbeam mode (μXANES), as well as XANES in full-field mode (FF-XANES), is used to examine the variation in sulfur chemistry of lazurite extracted from heat-treated lapis lazuli rock obtained from Afghanistan and five historical paint samples from 15th and 17th century Netherlandish paintings by Henri Bellechose, Jan Brueghel (II), Johan Maelwael, Jan Steen, and Rogier van der Weyden. The temperatures of treatment for the former are chosen on the basis of historical literature (*25*, *27*) and with consideration for earlier research performed on the heating of lazurite powders, denoting the potential for structural and compositional changes above ca. 500° to 550°C (*33*, *35*). The influence of heterogeneity that arises from heating a rock, the pastello extraction, and aging in the presence of oil is also considered. Together, the results reveal the potential of sulfur chemistry as a characteristic marker for heat treatment. Consequently, sulfur speciation may ultimately be a unique tool to probe the relation between pigment preparation and paint degradation.

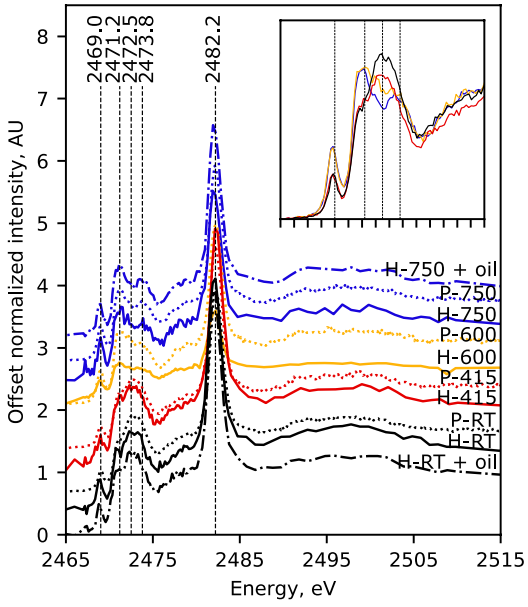

Fig. 1. Average XANES spectra of prepared pigment. Offset average normalized XANES spectra of lazurite extracted via the heavy-liquid (H-, solid lines) or pastello (P-, dotted lines) method from lapis lazuli following no heat treatment (i.e., RT, black lines) and heat treatment at 415°C (red lines), 600°C (yellow lines), and 750°C (blue lines). Furthermore, spectra of aged paint comprising linseed oil with either H-RT (black, dot-dashed line, H-RT + oil) or H-750 (blue, dot-dashed line, H-750 + oil). Spectra from pigment extracted via heavy-liquid and those from pigment extracted via pastello were gathered in full-field and unfocused XRF modes, respectively; for the former, spectra are the averages of spectra at all pixels corresponding to particles, and for the latter, spectra are the average of spectra acquired at three separate positions. Inset shows overlay of spectra from P-RT (black), P-415 (red), P-600 (yellow), and P-750 (blue) illustrating relative intensity changes with temperature.

RESULTS

Sulfur speciation in prepared pigments

For initial analysis, prepared pigments are considered as homogeneous, whereby bulk or averaged spectra per sample are used for between-sample comparisons. Sulfur K-edge unfocused- or FF-XANES spectra (averaged) of pigment prepared from lapis lazuli rock left at room temperature (RT) following either of two separation methods—pastello (P-RT) and heavy-liquid (H-RT)—are shown in Fig. 1 (dotted and solid lines, respectively). The latter method is assumed to be a physical process, not disrupting the chemistry of the minerals. Conversely, separation based on pastello is not well understood and is believed to proceed through a chemical process (*22*).

The P-RT and H-RT spectra demonstrate the general pattern for lazurite as found in the literature (*7*, *34*, *41*, *43*), with a relatively low-intensity peak at 2469.0 eV, an "envelope" of peaks between 2470.0 and 2475.6 eV, and a relatively high-intensity peak at 2482.2 eV. The lattermost peak has routinely been attributed to sulfate, while the assignments for the others have been the topic of much discussion (*7*, *33*, *34*). Conforming to the most recent literature, we attribute the peak at 2469.0 eV to contributions from di- and trisulfur radical species ($S2^{\bullet-}$ and $S3^{\bullet-}$, respectively) and the envelope to a combination of contributions from neutral, radical, and dianion sulfur species (*7*, *33*, *34*, *41*, *43*).

The relative contributions of these sulfur species to the overall spectral shape is fairly consistent with those observed for lazurite within untreated lapis lazuli rock obtained from Afghanistan in earlier reports with a maximum of the envelope near 2472.5 eV (*7*, *41*). Most notable, however, the similarity of the P-RT and H-RT in Fig. 1 to each other as well as to untreated rock (*41*) suggests that both the heavy-liquid and pastello—perceived as chemical in nature—separation methods have no apparent effect on the sulfur speciation; recently, Ganio *et al.* (*29*) investigated the subtle effects of the latter method. This similarity is unsurprising given that the sulfur species are trapped within the cages and thus inaccessible to external components from the separation methods.

On the other hand, XANES spectra of pigments separated via either method from lapis lazuli rock heated at 415°C (P-415 and H-415), 600°C (P-600 and H-600), or 750°C (P-750 and H-750) illustrate in Fig. 1 that sulfur speciation is dependent on the temperature of the rock heat treatment. While the spectral shapes of P-415 and H-415 are very similar to those of P-RT and H-RT, each with local maxima near the center of the envelope (between ca. 2472.5 and ca. 2473.8 eV), the shapes of XANES spectra for pigments from rock heated at 600° or 750°C have local maxima at 2471.2 and (lesser so) 2473.8 eV and minima at 2472.5 eV. In addition, there is a relative increase in the intensity of the peak at 2469.0 eV (Fig. 1, inset). Such an observation is consistent with previous reports noting structural and compositional modifications to lazurite at similar temperatures (*33*, *34*).

On the basis of the literature assignments, these spectral changes with temperature correspond to an increase in relative concentration

of the reduced sulfur species. More specifically, the increased intensities may be attributed to the di- and/or trisulfur radicals at 2469.0; the di-, tri-, and/or tetrasulfur radicals and/or dianions at the low-energy portion of the envelope (ca. 2470 to 2472 eV); and the tri- and/or tetrasulfur radicals and/or dianions at the high-energy portion of the envelope (ca. 2473 to 2475 eV); the relative contributions of each species at these energy ranges are more explicitly considered by Pascal *et al.* (*43*) Complementary to these, the relative decrease at the center of the envelope (ca. 2472.5 eV) may best be attributed to a decrease in relative contributions from neutral sulfur (S_8) species (*44*).

In addition, it was observed that the overall blue color of the lapis lazuli rock intensifies with heating (see fig. S1). As trisulfur radical species are responsible for the blue color of lazurite, (*9*, *10*, *19*–*21*, *11*–*18*) and have substantial peak contributions at 2469.0 eV and between ca. 2470 and 2472 eV, the spectral patterns observed for H-600 and H-750 (or P-600 and P-750) are consistent with an increase in relative concentration of trisulfur radicals and, in turn, with the visual color change observed in the rock upon increasing the temperature of heat treatment. It was also observed that cutting, grinding, milling, and separation via the pastello method were easier for heat-treated rock than for unheated rock, implying that other physical or chemical changes arise with heat treatment and are worthy of further study.

In a study involving the heating of lazurite powder in open and closed environments, Tauson *et al.* (*33*) and Fleet and Liu (*34*) similarly show a correlation between color change and XANES spectral pattern for natural and synthetic lazurite, respectively. Notably, a similar pattern to that seen for H-750 (or P-750) in Fig. 1 is reported by Tauson and coworkers (*33*) upon annealing coarse (>0.1 mm) lazurite powder in air (800°C for 1 day), which also intensified the color; annealing fine grains (0.01 to 0.03 mm) under the same conditions, however, led to a loss of blue color. There are instances where the spectrum of synthetic lazurite also shows similarity to this pattern (*7*, *34*) yet has characteristically less sulfate than lazurite from natural sources. Moreover, the most equivalent pattern of the envelope (2470.0 to 2475.6 eV) to that of H-750 (or P-750) in Fig. 1 is by Fleet and Liu (*34*) from synthetic powder after heating at 800°C for 1 day under vacuum.

To our knowledge, the present study is the first to report on the sulfur species present in ultramarine pigment from heat-treated rock rather than heat-treated powder. The present findings suggest that heating lazurite within a rock limits access of oxygen to the cages—much like coarse powder in air or fine (e.g., synthetic) powder under vacuum—favoring the formation of reduced over oxidized species with heating and resulting in the intensified blue color. Important as well, the "double-peak" pattern of the envelope observed for H-750 or P-750 (and H-600 or P-600, but less pronounced) is very dissimilar to those that may arise from lazurite of untreated lapis lazuli from the various natural sources (*41*) and from lazurite extracted at different stages of the pastello method (*29*). Together, these observations indicate that sulfur speciation provides a unique marker for lazurite extracted from heat-treated lapis lazuli rock.

Heterogeneity in prepared pigments

While in the above discussion samples were considered as homogeneous, heterogeneity was investigated on the heavy-liquid pigments using FF-XANES (*45*, *46*) to understand more intricately the influence of preparation method on natural ultramarine pigments. This technique consists of acquiring x-ray radiographs of the sample (in transmission), at a hundred energies below and above the absorption edge of interest (here, sulfur K-edge) (see details below). The full FF-XANES data from each sample therefore provide one XANES spectrum per radiograph pixel; hence, about 1 million to 4 million XANES spectra were collected per radiograph stack in a reasonable time. As a result, data interpretation is not biased by the selection of a few points of interest, as may be the case with standard μXANES, thereby allowing statistical consideration of heterogeneity.

Preliminarily, analysis of FF-XANES data was done on few individual pixels or in a qualitative way by measuring integrated intensity over specific energy region of interests. This revealed an increase in heterogeneity with increasing temperature of heat treatment. However, considering the very high number of pixels in FF-XANES, a statistical approach was then preferred. Attempts using principal component analysis (PCA) coupled with *k*-means clustering were ineffective at describing the preliminary findings. Alternatively, nonnegative matrix factorization (NMF) (*47*) was successfully used to decompose each normalized FF-XANES spectrum into main components (see Materials and Methods for further details).

The three NMF components obtained through analysis of H-750 spectra (Fig. 2A) show spectral patterns similar to those observed in the average spectra of Fig. 1, where the spectra of components 1 and 3 correlate well with those from averages of H-750 (or P-750) (representing the "double peak" envelope) and H-RT (or P-RT) (representing the "single peak" envelope) particles, respectively. In Fig. 2B, the pair plot of the NMF-derived coefficients for these components for each heavy-liquid pigment demonstrates a shift from higher relative coefficients in component 3 (i.e., single peak) to higher relative coefficients in component 1 (i.e., double peak) with increasing temperature of heat treatment, consistent with Fig. 1. The relation of the clusters further shows more similarity of H-RT (black, diamonds) and H-415 (red, circles) to each other than to H-600 (yellow, right-facing triangles) and H-750 (blue, top-facing triangles), H-750 most dissimilar to the others and more spread, and H-600 as intermediate.

Figure 2C presents FF-XANES images of the heavy-liquid separated pigments comprising pixels in false colors corresponding to the difference between the NMF-derived coefficients for components 3 and 1, with more positive (pale yellow) and negative (dark blue) values representing more contributions from components 3 and 1, respectively. Complementing Fig. 2B, comparison of the false-colored images of Fig. 2C shows decreasing contributions of component 3 (fewer pale yellow pixels)—the single peak envelope—with increasing temperature of treatment. Notably, comparison also reveals that relative heterogeneity increases with increasing temperature of heat treatment, corresponding to the increased spread for H-750 in Fig. 2B; because the finest grinding phase was performed first to produce H-750 and then continued in order of decreasing temperature of treatment, the observed heterogeneity cannot be an artifact of contamination from the reused vial. While images of H-RT and H-415 are composed almost entirely of pale yellow pixels, the image of H-750 is composed of pixels ranging over the entire false-color scale, demonstrating a range of spectral contributions from both components; again, H-600 falls intermediate between the others.

The heterogeneity appears to be present only between particles and not within particles, as demonstrated by spectra of neighboring pixels across individual particles (i and ii, indicated by arrows in Fig. 2C) of H-750 in Fig. 2D. Similar trends are observed for two other particles of H-750 (iii and iv) and for the other samples, as shown in fig. S2. The observation of in-particle homogeneity with

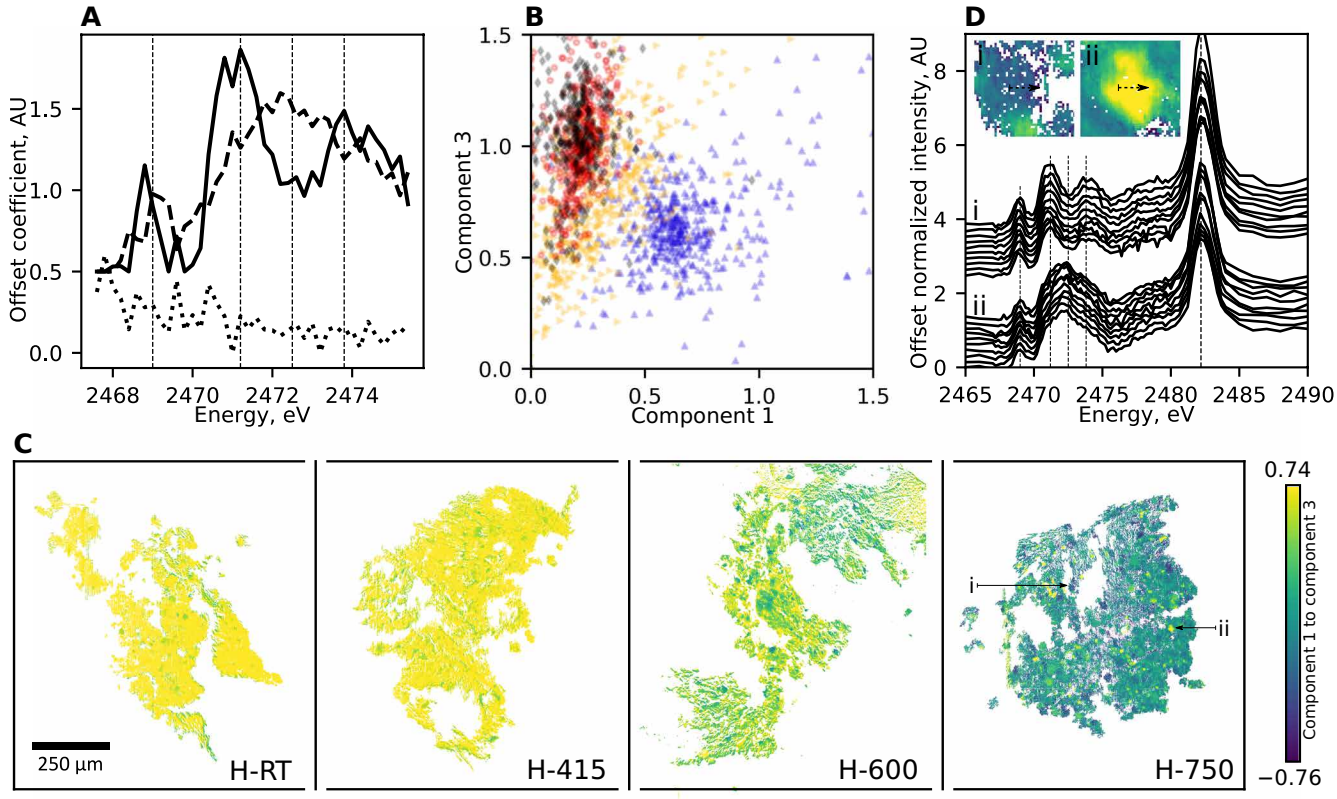

Fig. 2. Heterogeneity in prepared pigments observed with FF-XANES. (**A**) Components 1 (solid line), 2 (dotted line), and 3 (dashed line) resulting from performing NMF with three components on normalized FF-XANES spectra of H-750 particles over the energies shown. (**B**) Pair plot of NMF-derived coefficients for component 3 versus component 1 for normalized FF-XANES spectra of H-RT (black diamonds), H-415 (red circles), H-600 (yellow right-facing triangles), and H-750 (blue top-facing triangles) particles; each point represents every 1000th spectrum. (**C**) False-colored FF-XANES images of H-RT, H-415, H-600, and H-750, where each pixel corresponds to the difference between the NMF-derived coefficients for components 3 and 1. (**D**) Offset single-pixel normalized FF-XANES spectra of H-750 stepping pixel-by-pixel across (i) dark blue (upper curves) and (ii) pale yellow (lower curves) false-colored particles noted by the black arrows and corresponding those particles labeled in the H-750 image of (C). See fig. S2 for other examples.

between-particle heterogeneity may suggest a preference for lazurite mineral phases to separate at crystallographic phase boundaries upon grinding from rock to pigment powder; however, a more thorough investigation would be required to determine this explicitly.

Together, the observed heterogeneity and its dependence on temperature of treatment is perhaps unsurprising given that the heating is performed on solid pieces of rock open to air. As a rock, there exists an inherent gradient with respect to both temperature and access to oxygen from the surface to the core (*30*). Therefore, under the chosen experimental conditions, it can be inferred that the profiles from H-750 that parallel those from the low-temperature (or RT) treatments arise from regions of the rock where optimum conditions for changes in sulfur chemistry were not completely reached. In addition to temperature, the influence of heat treatment on lazurite can therefore be expected to depend on both the duration of heating and the size of the rock (i.e., the distance of lazurite from the rock surface).

Oil and aging of paint models

To further probe the potential for sulfur speciation as a marker for the heat treatment method, we tested the influence that aging oil may have on sulfur speciation. Models for historical paint comprising linseed oil with H-RT or H-750 were prepared and underwent accelerated aging for ca. 1 month following ca. 1 month of natural drying. Average spectra from FF-XANES acquisitions gathered on thin sections of these aged paint models (Fig. 1, dot-dashed lines) show no distinct differences from those of the corresponding raw pigments (Fig. 1, solid and dotted lines), and the relative heterogeneity is like that observed in the raw pigments (Fig. 2C), presented in fig. S3. Specifically, the relative ratios of the reduced to oxidized species remain consistent after mixing each pigment with oil and then following accelerated aging.

The consistent spectral profiles following aging demonstrate that sulfur speciation is not affected by mixing with oil and paint aging (under the studied conditions). More importantly, it directly reveals that the blue chromophore—assumed as the trisulfur radical—is not affected by aging with respect to other sulfur species, under the assumption that natural aging would not introduce external environmental factors other than light and humidity; for instance, an environment that introduces increased acidity is known to degrade the lazurite cages releasing the chromophore (*11*, *13*). Such an observation is in accordance with previous publications proposing that visual changes to an ultramarine paint surface are a result of changes in the oil network rather than the pigment itself (*25*, *48*, *49*).

Sulfur speciation in historical samples

With the sulfur signature uniquely dependent on the temperature of heat treatment, XANES at the sulfur K-edge shows promise as a

tool for identifying such treatment as applied during pigment preparation for historical paints. While the spectral patterns are indicative of the influence of heat on sulfur speciation within lazurite, the heterogeneity that results from the heating of lapis lazuli rock limits that which can be concluded concerning the treatment of the rock from which the lazurite pigment derives. More specifically, because the sulfur signature of lazurite from unheated lapis lazuli (i.e., single peak) remains present after heating, it provides no indication from a single particle as to the rock from which it came. In contrast, the double peak uniquely appears only following heat treatment; therefore, it provides a marker even from a single particle about the treatment of the rock from which it came.

The studied painting corpus contains five masterpieces (shown in Fig. 3) produced by major Netherlandish painters from the 15th and 17th centuries, namely, Johan Maelwael's *Pieta with the Holy Trinity*, ca. 1400 (Louvre, sample from blue on verso); Henri Bellechose's *The Last Communion and Martyrdom of Saint Denis*, 1416 (Louvre, sample from a blue garment); Rogier van der Weyden's *The Lamentation of Christ*, ca. 1460–1464 (Mauritshuis, sample from Mary's blue robe); Jan Brueghel (II)'s *Still Life with Flowers in a Glass*, ca. 1625–1630 (Rijksmuseum, sample from blue hyacinth on the right); and Jan Steen's *The Life of Man*, ca. 1665 (Mauritshuis, sample from blue garment of rightmost figure). Sample preparation and past analysis were performed by the C2RMF, the Mauritshuis, the RKD—Netherlands

Fig. 3. Images of the studied historical paintings. Visible images of the following paintings (counterclockwise from the top left): Johan Maelwael's *Pieta with the Holy Trinity*, ca. 1400, recto (Louvre), C2RMF/Jean-Louis Bellec; Henri Bellechose's *The Last Communion and Martyrdom of Saint Denis*, 1416 (Louvre), C2RMF/Jean-Louis Bellec; Rogier van der Weyden's *The Lamentation of Christ*, ca. 1460–1464 (Mauritshuis), Mauritshuis/Margareta Svensson; Jan Brueghel (II)'s *Still Life with Flowers in a Glass*, ca. 1625–ca. 1630 (Rijksmuseum), Rijksmuseum, Amsterdam; Jan Steen's *The Life of Man*, ca. 1665 (Mauritshuis), Mauritshuis/Margareta Svensson; Johan Maelwael's *Pieta with the Holy Trinity*, ca. 1400, verso (Louvre), C2RMF/Jean-Louis Bellec. Relative sizes have not been preserved. See fig. S4 for further details.

Institute for Art History, and the Rijksmuseum, as indicated in the Supplementary Materials. Spanning over 200 years, the set of paintings comes from three different institutions and includes five artists, three types of support (panel, canvas, and copper), and possibly two types of binding media (oil and mixed binder) (see fig. S4).

For each of the five paintings, μXANES spectra were acquired in x-ray fluorescence (XRF) mode with an attenuated focused microbeam at different locations on single lazurite particles and over several particles per sample (see technical details below). The acquisition locations were confidently selected on the lazurite pigment particles via the colocation of Si, Al, and S in μXRF maps (fig. S5). Average spectra per particle, whereby all individual spectra comprising the averages attained sufficient signal to noise, were then compared to those of the prepared pigment (four samples are displayed in fig. S6).

In all of the samples, some particles exhibited characteristic spectra for lazurite from heat-treated lapis lazuli, and a selection is shown in Fig. 4. Notably, these spectra have peaks of higher intensities at 2471.2 eV relative to those at both 2472.5 and 2473.8 eV, with those from Bellechose (Fig. 4A) and Maelwael (Fig. 4B) also exhibiting clear local minima at 2472.5 eV. The spectral similarity of these historical pigment particles to those from the pigments prepared from heat-treated lapis lazuli rock discussed above (e.g., H-750 and H-600; Fig. 1) strongly suggests that each of these artists used ultramarine pigment containing lazurite derived from heat-treated lapis lazuli rock.

Much like the prepared pigments, heterogeneity is also present in the historical samples. For instance, Fig. 5 (upper) exhibits average spectra for all of the lazurite particles measured in the paint cross-section from Johan Maelwael's *Pieta with the Holy Trinity* shown in the microscope image under ultraviolet light (lower); the exact locations of these spectral acquisitions are marked on the μXRF map in fig. S5. It can be observed that there are a variety of different spectral patterns, ranging from similar to H-750 (Fig. 5, spectra b and c), to H-600 (Fig. 5, spectrum h), to H-RT (Fig. 5, spectrum l). There appears to be a relative correlation in some particles between the intensity of the blue color and the relative contribution of the trisulfur radical species to the spectral profile, consistent with the discussion above and further evidence of similarities to the prepared pigments from heat treatments (recall fig. S1). Similar heterogeneity and correlation to pigment particle colors are also observed in the other historical samples (see figs. S5 and S6).

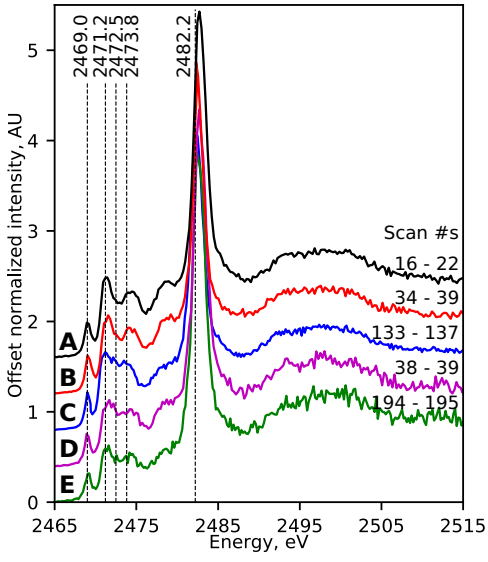

Fig. 4. Example μXANES spectra from lazurite within historical paint samples. Offset examples of average normalized μXANES (attenuated) spectra each from single lazurite particles in historical samples from (**A**) Henri Bellechose's *The Last Communion and Martyrdom of Saint Denis*, 1416 (Louvre); (**B**) Johan Maelwael's *Pieta with the Holy Trinity*, ca. 1400 (Louvre); (**C**) Jan Steen's *The Life of Man*, ca. 1665 (Mauritshuis); (**D**) Rogier van der Weyden's *The Lamentation of Christ*, ca. 1460–1464 (Mauritshuis); and (**E**) Jan Brueghel (II)'s *Still Life with Flowers in a Glass*, ca. 1625–ca. 1630 (Rijksmuseum). The scan numbers are those included in each average and correspond to the μXRF map in fig. S5.

DISCUSSION

We identify sulfur speciation within the lazurite cage as a reliable marker for the preparation of the ultramarine pigment from heat-treated

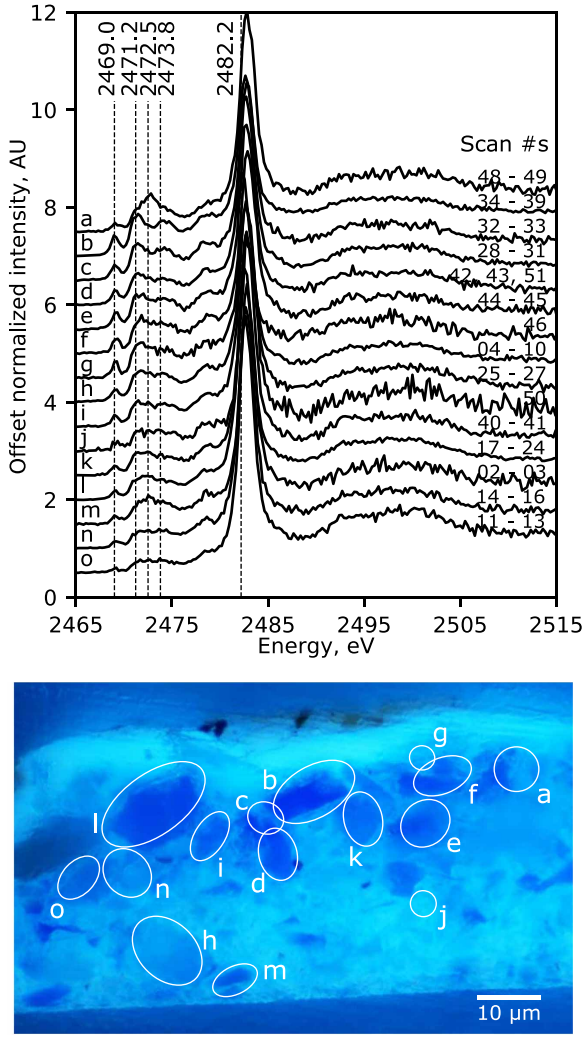

Fig. 5. μXANES spectra from individual lazurite particles within a historical paint sample. From Johan Maelwael's *Pieta with the Holy Trinity* from ca. 1400 (Louvre), offset average normalized μXANES (attenuated) spectra (upper) per particle as labeled in the paint cross-section (lower; C2RMF/Myriam Eveno) showing heterogeneity in the lazurite sulfur signals. The scan numbers are those included in each average and correspond to the μXRF map in fig. S5A. Spectrum "b" is the same as that shown in Fig. 4B.

lapis lazuli rock using μXANES and FF-XANES spectroscopy at the sulfur K-edge. While the sensitivity of the technique has already been established to assess geographical provenance of natural lazurite (*41*), the present work highlights a unique spectral pattern for pigment extracted from rock heated ≥600°C (for 1 hour), albeit not homogeneously distributed. Increasing heterogeneity was observed with increasing temperature of heat treatment, revealing that sulfur chemistry is likely influenced by the temperature and duration of heating and, in turn, also the size of the lapis lazuli rock. As a consequence, the presence of the unique pattern serves as a marker for heat treatment, while its absence leaves an ambiguous conclusion.

Sulfur K-edge XANES is noninvasively applicable to fragments from historical paintings but requires submicrometric resolution with attenuation and collection of spectra over and within many particles. This is important not only to mitigate risks of radiation damage but also as a consequence of heterogeneity observed in model samples. A systematic study of samples from five major Netherlandish historical paintings (ca. 1400–ca. 1665) revealed that artists were using ultramarine pigment extracted from rock after exposure to heat, whether it be during mining or post-mining treatments. While the motivation for the heat treatment—and its relation to mining practices—is not well documented in recipes, the correlation of this treatment to the intensified blue color of the resulting pigment is consistent with the historical desire to obtain the most intense blue ultramarine. However, the observation here that both the grinding of lapis lazuli and the extraction of lazurite therefrom are easier following heat treatment is also worthy of consideration for historical motivation, complementing the aim of fire setting.

The results of the current study contribute to our understanding of not only the use of the most valued pigment throughout history but also the influence of temperature on mineral phases. From a technical point of view, FF-XANES markedly enhances the number of spectra gathered per sample, thereby providing a means for unraveling relative contributions especially when coupled with statistical processing methods, like NMF. We aim to investigate further the implications of the altered mineral phase on the degradation of ultramarine blue paint. This has value well beyond cultural heritage, including in the studies of geological formations, such as the color of slag-based mortars and concretes (*50*), and the developments of sodium-sulfur batteries, where the monitoring of sulfur forms is crucial (*44*, *51*).

MATERIALS AND METHODS

Heat treatment and coarse grinding (*52*)

Lapis lazuli rock from the Sar-e-Sang region of Afghanistan was obtained from P. P. Pothoven (2014) and was cut into smaller pieces using a diamond circular saw (16 pieces, ca. 150 to 190 g each). Two pieces were put aside and left at RT, and the other pieces were heated in the CEM Corporation Microwave Ashing System-300 (USA) at either 415°, 600°, or 750°C for 1 hour after reaching the designated temperature. Lapis lazuli rock from each temperature variant was placed in a bucket with cold water to cool. After cooling, each rock piece was cut into smaller pieces using a diamond circular saw, followed by crushing to a particle size smaller than 200 μm in a jaw crusher with tungsten carbide plates; components were cleaned before each sample using a vacuum, ethanol, and compressed air. The lapis lazuli powder for each temperature variant was sieved (20 μm mesh) with water to remove very fine dust; sieves were cleaned in the same method as other components with the addition of an ultrasonic bath before ethanol rinsing.

Extraction of lazurite via heavy-liquid separation (*52*)

A portion of each temperature variant of the lapis lazuli powder (particle sizes, 20 to 200 μm) was treated in a heavy-liquid procedure in an overflow centrifuge (LOC 50 separator) developed at the Vrije Universiteit Amsterdam (*52*) to produce three fractions each. Mixtures of diiodomethane (D = 3.32 g cm^{-3}) and dichlorobenzene (D = 1.30 g cm^{-3}) were used to prepare three fractions: low (d < 2.38 g cm^{-3}), mid [2.38 g cm^{-3} < d < 2.45 g cm^{-3}, the density range given for natural lazurite (*53*)], and high (d > 2.45 g cm^{-3}) density. The three fractions of each were subsequently sieved to obtain fractions of the following particles sizes: 20 to 30, 30 to 60, 60 to 90, 90 to 120, 120 to 160, and 160 to 200 μm.

Lazurite fractions (mid density, particle sizes <120 μm) of each temperature variant (from high to low) were further ground in batches (1 g each) for 10 min to particle sizes of approximately 0.5 to 1.0 μm [verified by transmission electron microscopy (TEM); fig. S8] using two agate balls and an agate vial via the 8000M Mixer/Mill High-Energy Ball Mill. Between fractions, agate components were sonicated in water; rinsed with deionized (DI) water, ethanol, and acetone; and dried in an oven. In some instances, components were also cleaned by grinding two batches of quartz for 5 to 10 min each to remove trace blue powder followed by rinsing steps again. The resultant fractions are referred to as the heavy-liquid pigments throughout the article.

Extraction of lazurite via pastello separation

A separate portion of each temperature variant of the lapis lazuli powder (particle sizes, 20 to 200 μm) was reduced further in size using a vibrating cup mill (Fritsch, Pulverisette 9) for 21 s and subsequently milled in an agate planetary mill (Fritsch, Pulverisette 5) containing five agate milling balls for 45 min to obtain an average particle size often found in paintings [calculated from observations reported in the thesis of Klaas (*25*)]; the respective mills did not exceed temperatures of 25° and 40°C. The particle size distributions were measured with a HELOS KR laser particle size analyzer from Sympatec for the four temperature variants, with means and medians ranging from 6.8 to 7.2 μm and 6.8 to 11 μm, respectively.

Dough known as pastello was prepared as a mixture of mastic (53 g), colophonium (33 g), beeswax (24 g), and linseed oil (15 g); all materials were acquired from de Kat, The Netherlands. The lapis lazuli powders were added into the pastello with a powder:pastello weight ratio of 1:1.35. The powder-containing pastellos were then divided into smaller portions (approximately 30 g each), stored for 15 days in DI water, and then each kneaded for 3 hours in DI water (1.3 liters). Following kneading, the resultant fine blue powder was allowed to settle and collected by decanting off the water. Remaining water was left to evaporate at ambient conditions. The resultant fractions are referred to as the pastello pigments throughout the article.

Transmission electron microscopy

Heavy-liquid extracted lazurite from lapis lazuli rock kept at RT and that treated at 750°C was analyzed with TEM by AkzoNobel (Deventer, The Netherlands). The loose pigments were embedded in epoxy-thiol resin and microtomed to thin slices (ca. 100 nm) at

RT. The sections were collected onto carbon-coated copper TEM grids and studied using a JEOL 2010F FEG-TEM at 200 kV. Particles were determined to have lengths between 500 nm and 1 μm with an aspect ratio of approximately 1:3 (fig. S8).

Paint model preparation and aging

Models for historical paints were prepared using heavy-liquid extracted lazurite pigments from lapis lazuli rock kept at RT and that treated at 750°C. Linseed oil [cold-pressed from Sweden, #73020 from Kremer Pigments, Chemical Abstracts Service (CAS) no. 8001-26-1] was added to each lazurite fraction (53% w/w in pigment) on an automatic muller comprising two parallel glass plates and gently mixed together. Twice, the paint was then further mixed with 25 turns of the upper plate atop the lower (under a weight of 10 kg) and consolidated at the center of one plate with a palette knife. Mixed paint was deposited on Melinex polyester wrap (250 μm thick, #M026 from www.labshop.nl) and drawn into a thin strip with a drawdown bar (50 μm height). Paintouts were set to dry vertically under laboratory conditions for approximately 1 month followed by 1 month of accelerated aging in a Xenotest (daylight, 40% relative humidity, ca. 50°C).

Historical paint samples

Samples were gathered from blue-colored regions of five paintings held in collections of the Louvre (Paris, France), the Mauritshuis (The Hague, The Netherlands), and the Rijksmuseum (Amsterdam, The Netherlands) by four institutions; see section above and in fig. S4.

Pigment and paint cross-section preparation and imaging

The loose pigments extracted from lapis lazuli and model paint samples were embedded in Technovit 2000 LC (a methyl methacrylate resin; Heraeus Kulzer GmbH, Germany) and cured under blue light. Each embedded cross-section was then dry-polished with Micro-Mesh polishing papers (until finest of 12,000 grit; Micro-Surface Finishing Products Inc., Wilton, IA, USA) to expose the sample. Lens paper was used to wipe the sample surfaces of polishing residue before analysis. The polished cross-sections from historical paintings were similarly embedded and polished, and each was imaged under ultraviolet illumination (see the Supplementary Materials for details).

Synchrotron-based measurements

At the European Synchrotron Radiation Facility (ESRF), sulfur K-edge XANES spectra were collected using beamline ID21 (*38*). Samples were mounted within a vacuum chamber, and x-rays were generated by an undulator. X-ray energy was scanned across the sulfur K-edge using a fixed-exit Si (111) double-crystal monochromator (calibrated by fixing the maximum absorption of gypsum at 2.48239 keV).

Spectra were gathered in either an XRF or a transmission configuration. For the former, first XRF maps were collected with an incident x-ray energy of 2.5 keV either (i) without using focusing optics, in an unfocused mode with the x-ray beam narrowed to a spot size of around 100 μm diameter using a pinhole (flux of 3×10^9 photon s^{-1}), or (ii) with focusing optics, to reduce the x-ray beam to a submicrometric spot size of 0.6×1.0 μm^2 (flux of 4.3×10^8 photons s^{-1}, attenuated using a 6-μm aluminum filter), with the latter referred to as μXRF. The unfocused mode was used for the bulk study of some lazurite powder materials, while the attenuated focused mode was necessary to probe individual pigment particles (usually dispersed in a lead-based matrix) in historical samples. Points of interest were chosen over the samples based on the Al, Si, and S distribution in these maps, and XANES or μXANES spectra were collected using unfocused or attenuated focused beam, respectively. In focused mode without attenuation, photoradiation damage (*7*, *29*, *54*) was observed during consecutive μXANES acquisition (see the Supplementary Materials and fig. S7 for further details). Decreasing the flux using attenuators and accumulating single spectra from several points per pigment particle was implemented as a mitigation. Besides, to evaluate pigment heterogeneity, analyses were performed over several (>10) particles per historical sample. All XANES spectra were acquired by scanning the energy from 2.46 to 2.53 keV.

The so-called FF-XANES setup was used for the two-dimensional XANES study of the lazurite pigments and artificially aged model paints. In this configuration, x-ray radiographs of the sample [powders were spread over sulfur-free XRF tape (Fluxana), while model paints were sliced as 10-μm-thin sections via microtoming and held with Ultralene foil] are acquired with a large, unfocused beam (~1×1 mm^2). A scintillator (Lu_2SiO_5:Tb, 10 μm thick) was placed a few millimeters downstream from the sample, and a 10× optical objective was used to magnify the image onto a complementary metal oxide semiconductor (CMOS) PCO.edge camera, giving a pixel size of 0.7×0.7 μm^2 and a spatial resolution in the order of micrometers. Further instrumental details are given by Cotte *et al.* (*38*).

Data processing and statistical analysis

Data processing was performed using several open-source software packages. For XRF maps and XANES spectra gathered in XRF mode, the PyMca (*55*) software was used for batch fitting, in particular to separate the S L-line from the Pb M-lines in historical samples supplemented with Python script (https://github.com/woutdenolf/spectrocrunch). For FF-XANES, radiograph alignment was achieved using Silx (https://github.com/silx-kit/silx).

Normalization of all (unfocused, μ, and FF) XANES spectra [pre-edge to 0 arbitrary units (AU) and post-edge to 1 AU] was accomplished using PyMca (version 5.4.0) (*55*). However, this process led to a loss of some pixels in the instance of FF-XANES: In this mode, spectra are acquired in transmission, leading to decreased sensitivity for sulfur species and less optimum batch normalization results than in XRF mode.

Image manipulation (in particular, production of masks for FF-XANES) was achieved in GIMP (2.10.8). All other processing was performed via Python (3.6.5) using standard scientific packages (e.g., pandas, NumPy, Matplotlib, and seaborn), and figures were compiled in Inkscape (0.92). Of note, subtle differences in energies between beamtimes were corrected by calibrating all lazurite prepeaks to 2469.00 eV, and FF-XANES average spectra were calculated over all pixels representing pigment using a mask.

NMF (*47*) was used using the Python package scikit-learn (*56*). Unlike PCA, NMF provides a parts-based representation of the data through the constraint that the parts (or components) must be nonnegative. While NMF is more applicable to XANES and many other spectral data, it still appears underused in the literature. As detailed above, heterogeneity increases with increasing temperature of heat treatment; therefore, decision was taken to perform NMF on H-750 spectra, from 2467.60 to 2475.60 eV, using three components; the number of components was chosen to be the lowest that described heterogeneities observed with qualitative region-of-interest measurements. The FF-XANES spectra for all samples were then decomposed on the basis of these three components, and false-colored maps were

produced of their absolute and relative proportions. Details of data processing are provided in Jupyter Notebook sheets available on GitHub at https://github.com/alessaan/rhapsody-in-blue, and all raw, preprocessed, and processed XANES data files are available at doi:10.15151/ESRF-DC-186933507.

SUPPLEMENTARY MATERIALS

Supplementary material for this article is available at http://advances.sciencemag.org/cgi/content/full/6/18/eaay8782/DC1

REFERENCES AND NOTES

1. J. Plesters, in *Artists' Pigments: A Handbook of Their History and Characteristics, vol. 2*, A. Roy, Ed. (National Gallery of Art, 1993), pp. 37–65.
2. R. J. Gettens, G. L. Stout, *Painting Materials: A Short Encyclopaedia* (Dover Publications Inc., 1966).
3. J. Wyart, P. Bariand, J. Filippi, Lapis-Lazuli from Sar-e-Sang. *Gems Gemol.* **Winter**, 184–190 (1981).
4. G. Herrmann, Lapis lazuli: The early phases of its trade. *Iraq* **30**, 21–57 (1968).
5. M. Casanova, in *South Asian Archaeology, 1989: Papers from the Tenth International Conference of South Asian Archaeologists in Western Europe, Musée National Des Arts Asiatiques-Guimet, Paris, France, 3-7 July 1989* (Prehistory Press, 1992), pp. 49–55.
6. N. Eastaugh, V. Walsh, T. Chaplin, R. Siddall, *Pigment Compendium: A Dictionary of Historical Pigments* (Elsevier Butterworth-Heinemann, 2004).
7. J. Goettlicher, A. Kotelnikov, N. Suk, A. Kovalski, T. Vitova, R. Steininger, Sulfur K X-ray absorption near edge structure spectroscopy on the photochrome sodalite variety hackmanite. *Z. Krist.* **228**, 157–171 (2013).
8. N. Bolotina, Forms and origin of structure modulation in lazurites. *Philos. Mag.* **87**, 2679–2685 (2007).
9. R. J. H. Clark, M. L. Franks, The resonance Raman spectrum of ultramarine blue. *Chem. Phys. Lett.* **34**, 69–72 (1975).
10. R. J. H. Clark, D. G. Cobbold, Characterization of sulfur radical anions in solutions of alkali polysulfides in dimethylformamide and hexamethylphosphoramide and in the solid state in ultramarine blue, green, and red. *Inorg. Chem.* **17**, 3169–3174 (1978).
11. E. Del Federico, W. Shöfberger, J. Schelvis, S. Kapetanaki, L. Tyne, A. Jerschow, Insight into framework destruction in ultramarine pigments. *Inorg. Chem.* **45**, 1270–1276 (2006).
12. B. Ledé, A. Demortier, N. Gobeltz-Hautecœur, J.-P. Lelieur, E. Picquenard, C. Duhayon, Observation of the v_3 Raman band of S_3^- inserted into sodalite cages. *J. Raman Spectrosc.* **38**, 1461–1468 (2007).
13. E. Del Federico, W. Shoefberger, R. Kumar, W. Ling, S. M. Kapetanaki, J. Schelvis, A. Jerschow, Solid-State NMR and resonance Raman studies of ultramarine pigments, *Mater. Res. Soc. Symp. Proc.* **852(OO5.4)**, 247–254 (2004).
14. R. J. H. Clark, T. J. Dines, M. Kurmoo, On the nature of the sulfur chromophores in ultramarine blue, green, violet, and pink and of the selenium chromophore in ultramarine selenium: Characterization of radical anions by electronic and resonance raman spectroscopy and the determination of their excited-state geometries. *Inorg. Chem.* **22**, 2766–2772 (1983).
15. D. Reinen, G.-G. Lindner, The nature of the chalcogen colour centres in ultramarine-type solids. *Chem. Soc. Rev.* **28**, 75–84 (1999).
16. S. D. Mclaughlan, D. J. Marshall, Paramagnetic resonance of sulfur radicals in synthetic sodalites. *J. Phys. Chem.* **74**, 1359–1363 (1970).
17. D. Arieli, D. E. W. Vaughan, D. Goldfarb, New synthesis and insight into the structure of blue ultramarine pigments. *J. Am. Chem. Soc.* **126**, 5776–5788 (2004).
18. A. Baranowski, M. Dębowska, K. Jerie, A. Jezierski, M. Sachanbiński, Ultramarine, lazurite, and sodalite studied by positron annihilation and EPR methods. *Acta Phys. Pol. A* **88**, 29–41 (1995).
19. N. Gobeltz-Hautecoeur, A. Demortier, B. Lede, J. P. Lelieur, C. Duhayon, Occupancy of the sodalite cages in the blue ultramarine pigments. *Inorg. Chem.* **41**, 2848–2854 (2002).
20. R. Steudel, Inorganic polysulfides S_n^{2-} and radical anions $S_n^{\cdot-}$. *Top. Curr. Chem.* **231**, 127–152 (2003).
21. T. Chivers, P. J. W. Elder, Ubiquitous trisulfur radical anion: Fundamentals and applications in materials science, electrochemistry, analytical chemistry and geochemistry. *Chem. Soc. Rev.* **42**, 5996–6005 (2013).
22. M. Favaro, A. Guastoni, F. Marini, S. Bianchin, A. Gambirasi, Characterization of lapis lazuli and corresponding purified pigments for a provenance study of ultramarine pigments used in works of art. *Anal. Bioanal. Chem.* **402**, 2195–2208 (2012).
23. C. d'A. Cennini, in *The Craftman's Handbook "Il Libro dell'Arte"*, D. V. Thompson Jr., Ed. (Dover Publications Inc., 1960), pp. 36–39.
24. H. Berke, The invention of blue and purple pigments in ancient times. *Chem. Soc. Rev.* **36**, 15–30 (2007).
25. J. Klaas, thesis, Technical University Munchen, Munchen, Germany (2011).
26. A. Kurella, I. Strauss, Lapislazuli und natürlliches Ultramarine. *Maltechnik-Restauro.* **89**, 34–54 (1983).
27. M. P. Merrifield, *Original Treatises: Dating from the XIIth to XVIIIth Centuries on the Arts of Painting, in Oil, Miniature, Mosaic, and on Glass; of Gilding, Dyeing, and the Preparation of Colours and Artificial Gems; Preceded by General Introduction; with Translations* (John Murray, 1849).
28. Florence, Biblioteca Laurenziana, Ms Ashburnhamia 349 fols. 53v - 54v, 81r - 83r.
29. M. Ganio, E. S. Pouyet, S. M. Webb, C. M. Schmidt Patterson, M. S. Walton, From lapis lazuli to ultramarine blue: Investigating Cennino Cennini's recipe using sulfur K-edge XANES. *Pure Appl. Chem.* **90**, 463–475 (2018).
30. G. Weisgerber, L. Willies, The use of fire in prehistoric and ancient mining: Firesetting. *Paléorient* **26**, 131–149 (2000).
31. C. R. Darwin, *The Expression of the Emotions in Man and Animals* (John Murray, 1872), p. 171.
32. V. L. Tauson, A. N. Sapozhnikov, E. V. Kaneva, S. V. Lipko, Reversion of incommensurate modulation in Cubic Lazurite: Example of reversible forced equilibrium? *Nat. Resour.* **5**, 761–771 (2014).
33. V. L. Tauson, J. Goettlicher, A. N. Sapozhnikov, S. Mangold, E. E. Lustenberg, Sulphur speciation in lazurite-type minerals (Na,Ca)8[Al6Si6O24](SO4,S)2 and their annealing products: A comparative XPS and XAS study. *Eur. J. Mineral.* **24**, 133–152 (2012).
34. M. E. Fleet, X. Liu, X-ray absorption spectroscopy of ultramarine pigments: A new analytical method for the polysulfide radical anion S_3^- chromophore. *Spectrochim. Acta Part B* **65**, 75–79 (2010).
35. V. L. Tauson, A. N. Sapozhnikov, S. N. Shinkareva, E. E. Lustenberg, The nature of the stability of an incommensurate 3D structural modulation in Baikal lazurite: Experimental data at 550 C. *Geochem. Int.* **47**, 815–830 (2009).
36. C. Miliani, A. Daveri, B. G. Brunetti, A. Sgamellotti, CO_2 entrapment in natural ultramarine blue. *Chem. Phys. Lett.* **466**, 148–151 (2008).
37. D. C. Koningsberger, R. Prins, *X-ray Absorption: Principles, Applications, Techniques of EXAFS, SEXAFS, and XANES* (Wiley, 1988).
38. M. Cotte, E. Pouyet, M. Salomé, C. Rivard, W. De Nolf, H. Castillo-Michel, T. Fabris, L. Monico, K. Janssens, T. Wang, P. Sciau, L. Verger, L. Cormier, O. Dargaud, E. Brun, D. Bugnazet, B. Fayard, B. Hesse, A. E. Pradas del Real, G. Veronesi, J. Langlois, N. Balcar, Y. Vandenberghe, V. A. Solé, J. Kieffer, R. Barrett, C. Cohen, C. Cornu, R. Baker, E. Gagliardini, E. Papillon, J. Susini, The ID21 X-ray and infrared microscopy beamline at the ESRF: Status and recent applications to artistic materials. *J. Anal. At. Spectrom* **32**, 477–493 (2017).
39. I. Osticioli, N. F. C. Mendes, A. Nevin, F. P. S. C. Gil, M. Becucci, E. Castellucci, Analysis of natural and artificial ultramarine blue pigments using laser induced breakdown and pulsed Raman spectroscopy, statistical analysis and light microscopy. *Spectrochim. Acta Part A* **73**, 525–531 (2009).
40. G. D. Smith, R. J. Klinshaw II, The presence of trapped carbon dioxide in lapis lazuli and its potential use in geo-sourcing natural ultramarine pigment. *J. Cult. Herit.* **10**, 415–421 (2009).
41. A. A. Gambardella, C. M. Schmidt Patterson, S. M. Webb, M. S. Walton, Sulfur K-edge XANES of lazurite: Toward determining the provenance of lapis lazuli. *Microchem. J.* **125**, 299–307 (2016).
42. M. E. Fleet, X. Liu, S. L. Harmer, H. W. Nesbitt, Chemical state of sulfur in natural and synthetic lazurite by S K-edge XANES and X-ray photoelectron spectroscopy. *Can. Mineral.* **43**, 1589–1603 (2005).
43. T. A. Pascal, C. D. Pemmaraju, D. Prendergast, X-ray spectroscopy as a probe for lithium polysulfide radicals. *Phys. Chem. Chem. Phys.* **17**, 7743–7753 (2015).
44. T. A. Pascal, K. H. Wujcik, J. Velasco-Velez, C. Wu, A. A. Teran, M. Kapilashrami, J. Cabana, J. Guo, M. Salmeron, N. Balsara, D. Prendergast, X-ray absorption spectra of dissolved polysulfides in lithium-sulfur batteries from first-principles. *J. Phys. Chem. Lett.* **5**, 1547–1551 (2014).
45. B. Fayard, E. Pouyet, G. Berruyer, D. Bugnazet, C. Cornu, M. Cotte, V. De Andrade, F. Di Chiaro, O. Hignette, J. Kieffer, T. Martin, E. Papillon, M. Salomé, V. A. Sole, The new ID21 XANES full-field end-station at ESRF. *J. Phys. Conf. Ser.* **425**, 192001 (2013).
46. V. De Andrade, J. Susini, M. Salomé, O. Beraldin, C. Rigault, T. Heymes, E. Lewin, O. Vidal, Submicrometer hyperspectral X-ray imaging of heterogeneous rocks and geomaterials: Applications at the Fe K-edge. *Anal. Chem.* **83**, 4220–4227 (2011).
47. D. D. Lee, H. S. Seung, Learning the parts of objects by non-negative matrix factorization. *Nature* **401**, 788–791 (1999).
48. K. Keune, F. Hoogland, J. Boon, D. Peggie, C. Higgitt, Comparative study of the effect of traditional pigments on artificially aged oil paint systems using complementary analytical techniques, in *15th Triennal Meeting of ICOM Committee for Conservation* (Allied Publishers Pvt. Ltd., 2008), pp. 833–842.
49. E. R. de la Rie, A. Michelin, M. Ngako, E. Del Federico, C. Del Grosso, Photo-catalytic degradation of binding media of ultramarine blue containing paint layers: A new perspective on the phenomenon of "ultramarine disease" in paintings. *Polym. Degrad. Stab.* **144**, 43–52 (2017).

50. M. Chaouche, X. X. Gao, M. Cyr, M. Cotte, L. Frouin, On the origin of the blue/green color of blast-furnace slag-based materials: Sulfur K-edge XANES investigation. *J. Am. Ceram. Soc.* **100**, 1707–1716 (2017).
51. R. Steudel, Y. Steudel, Polysulfide chemistry in sodium-sulfur batteries and related systems—A computational study by G3X(MP2) and PCM calculations. *Chem. A Eur. J.* **19**, 3162–3176 (2013).
52. L. Ijlst, New diluents in heavy liquid mineral separation and an improved method for the recovery of the liquids from the washings. *Am. Mineral.* **58**, 1084–1087 (1973).
53. A. N. Sapozhnikov, E. V. Kaneva, D. I. Cherepanov, L. F. Suvorova, V. I. Levitsky, L. A. Ivanova, L. Z. Reznitsky, Vladimirivanovite, $Na_6Ca_2[Al_6Si_6O_{24}](SO_4,S_3,S_2,Cl)_2 \cdot H_2O$, a new mineral of sodalite group. *Geol. Ore Depos.* **54**, 557–564 (2012).
54. M. Wilke, P. J. Jugo, K. Klimm, J. Susini, R. Botcharnikov, S. C. Kohn, M. Janousch, The origin of S4+ detected in silicate glasses by XANES. *Am. Mineral.* **93**, 235–240 (2008).
55. V. A. Solé, E. Papillon, M. Cotte, P. Walter, J. Susini, A multiplatform code for the analysis of energy-dispersive X-ray fluorescence spetra. *Spectrochim. Acta Part B* **62**, 63–68 (2007).
56. F. Pedregosa, G. Varoquaux, A. Gramfort, V. Michel, B. Thirion, O. Grisel, M. Blondel, P. Prettenhofer, R. Weiss, V. Dubourg, J. Vanderplas, A. Passos, D. Cournapeau, M. Brucher, M. Perrot, E. Duchesnay, Scikit-learn: Machine learning in Python. *J. Mach. Learn. Res.* **12**, 2825–2830 (2011).

Acknowledgments: We thank AzkoNobel for funding, of which A.A.G. gives additional thanks to T. Davies for support and B. Rossenaar for TEM analyses. XANES experiments were performed on beamline ID21 at the ESRF, Grenoble, France (experiments HG62, HG94, and HG139); we are grateful to A. Solé for providing assistance with PyMca, A. Gotz for reviewing Jupyter notebooks and assisting with the DOI, and A. de Maria for editing the DOI. M.C. thanks the KNAW for supporting her stays in The Netherlands through the Descartes Huygens prize. We are indebted to P. P. Pothoven for providing the lapis lazuli rock, and the Louvre (Paris, France) and the Mauritshuis (The Hague, The Netherlands) for the study of their paintings. For providing the embedded cross-sections and corresponding microscope images of historical samples, additional thanks are given to the C2RMF (Paris, France) for the Maelwael and Bellechose samples; the Mauritshuis (The Hague, The Netherlands)—in particular, S. Meloni—for the Steen sample; and the RKD—Netherlands Institute for Art History (The Hague, The Netherlands)—in particular, the archive of J. R. J. van Asperen de Boer—for the Van der Weyden sample. For imaging the Breughel sample, thanks are given to N. de Keyser of the Rijksmuseum. We also give thanks to the Cultural Heritage Agency of The Netherlands (Amersfoort, The Netherlands) for providing Xenotest chambers and the automatic muller (on permanent loan from Old Holland) as well as to I. Kneepkens, E. van Rietschoten, N. Kollard, J. Rosier, S. Matveev, and P. P. Pothoven for assistance with the pastello treatment. We are additionally grateful for support from the following: G. Albertson, N. de Keyser, G. de Vivo, E. Hermens, A. Krekeler, S. Smelt, B. van Driel, and R. van Langh of the Rijksmuseum; S. Meloni, C. Pottasch, A. Vandivere, and L. d'Hont of the Mauritshuis; F. Meirer of Utrecht University; and J. Rosier and N. Bergman of Vrije Universiteit Amsterdam. **Funding:** This work was supported by AkzoNobel (The Netherlands). **Author contributions:** The manuscript includes contributions of all authors. K.S., P.D.I., and K.K.: initial hypothesis; A.A.G., K.S., R.v.E., A.W., and K.K.: pigment preparation; A.A.G.: model paint preparation; A.A.G., V.G., and M.E.: paint sample selection; A.A.G., M.C., K.S., W.d.N., V.G., and K.K.: experimental XANES work; A.A.G., W.d.N., R.E., M.C., and V.G.: data processing; A.A.G., M.C., K.S., and K.K.: data interpretation. The manuscript is written by A.A.G. and edited by M.C. and K.K. and, to a lesser extent, all other authors; K.K. supervised the project. All authors have given approval to the final version of the manuscript. **Competing interests:** The authors declare that they have no competing interests. **Data and materials availability:** All data needed to evaluate the conclusions in the paper are present in the paper and/or the Supplementary Materials. Raw, preprocessed, and processed datasets are available at doi:10.15151/ESRF-DC-186933507, and data processing steps can be found in the GitHub repository, https://github.com/alessaan/rhapsody-in-blue. Additional data related to this paper may be requested from the authors.

Submitted 26 July 2019
Accepted 5 February 2020
Published 1 May 2020
10.1126/sciadv.aay8782

Citation: A. A. Gambardella, M. Cotte, W. de Nolf, K. Schnetz, R. Erdmann, R. van Elsas, V. Gonzalez, A. Wallert, P. D. Iedema, M. Eveno, K. Keune, Sulfur K-edge micro- and full-field XANES identify marker for preparation method of ultramarine pigment from lapis lazuli in historical paints. *Sci. Adv.* **6**, eaay8782 (2020).

Science Advances

Sulfur K-edge micro- and full-field XANES identify marker for preparation method of ultramarine pigment from lapis lazuli in historical paints

Alessa A. Gambardella, Marine Cotte, Wout de Nolf, Kokkie Schnetz, Rob Erdmann, Roel van Elsas, Victor Gonzalez, Arie Wallert, Piet D. Iedema, Myriam Eveno and Katrien Keune

Sci Adv **6** (18), eaay8782.
DOI: 10.1126/sciadv.aay8782